Hamiltonian Maps and Transport in Structured Fluids

Jeffrey B. Weiss*

National Center for Atmospheric Research

P.O. Box 3000

Boulder, CO 80307

Structures such as waves, jets, and vortices have a dramatic impact on the transport properties of a flow. Passive tracer transport in incompressible two-dimensional flows is described by Hamiltonian dynamics, and, for idealized structures, the system is typically integrable. When such structures are perturbed, chaotic trajectories can result which can significantly change the transport properties. It is proposed that the transport due to the chaotic regions can be efficiently calculated using Hamiltonian mappings designed specifically for the structure of interest. As an example a new map is constructed, appropriate for studying transport by propagating isolated vortices. It is found that a perturbed vortex will trap fluid parcels for varying lengths of time, and that the distribution of such trapping times has slopes which are independent of the amplitudes of both the vortex and the perturbation.

August 1993

to be published in Physica D

Proceedings of the NATO and EGS Workshop on

Chaotic Advection, Tracer Dynamics, and Turbulent Dispersion

Sereno Di Gavi, Italy, May 1993.

* *current address*: Program in Atmospheric and Oceanic Sciences, Department of Astrophysics, Planetary, and Atmospheric Sciences, Campus Box 311, University of Colorado, Boulder, CO 80309

I. Introduction

Many fluid flows are highly structured, containing a variety of vortices, waves, jets, and fronts. These structures can exist over an extremely wide range of parameter values, from nonturbulent flows with relatively weak forcing such as Rayleigh-Benard convection beyond the first bifurcation, to extremely turbulent flows such as planetary atmospheres and oceans. Structures can have a profound impact on the transport properties of flows through a variety of mechanisms; jets can act as barriers to transport, while vortices and waves can trap fluid parcels and carry them large distances. These phenomena are of great importance in geophysical flows. The Gulf Stream can act as a barrier to transport, affecting both heat and salinity transport in the North Atlantic [1], the stratospheric polar night vortex traps fluid within its boundaries where chemical reactions result in ozone depletion [2], and vortices in the ocean can carry water far from its original source affecting the overall transport in the ocean [3, 4].

Studying the transport properties of a fluid requires the use of two different descriptions of a flow. The Eulerian description specifies the fluid properties (velocity, temperature, etc.) in a fixed reference frame, while the Lagrangian description specifies properties in a frame moving with each fluid parcel. The Eulerian velocity is $\vec{u}_E(\vec{x}, t)$ where $\vec{x}$ can be, for example, a position fixed in the frame of the laboratory for a laboratory experiment, or a position fixed to the Earth for a geophysical flow. Lagrangian properties are determined by $\vec{X}(\vec{x}_0, t)$, the position at time t of the fluid parcel labeled by its initial position $\vec{x}_0$, $\vec{X}(\vec{x}_0, 0) \equiv \vec{x}_0$. The relationship between the two descriptions is the fact that an ideal fluid parcel is transported by the local Eulerian velocity,

$$d\vec{X}/dt = \vec{u}_E(\vec{X}, t). \tag{1}$$

In this paper we shall only be concerned with the transport of ideal passive tracers that are described by (1). Real contaminants may have other forces acting on them such as drag or buoyancy which modify the relation (1). These effects are addressed by other contributions in this volume. Another simplification we shall make is that we only consider two-dimensional flows. Many geophysical flows are constrained by rapid rotation and stable stratification, resulting in flows which are approximately two-dimensional. In addition,

some laboratory flows have a symmetry which makes them effectively two-dimensional. The question of extension to three dimensions is certainly interesting, but we defer it to later work. In section II of this paper we discuss the general notion of using Hamiltonian maps to study transport. In section III we introduce a new map to study the geophysically important phenomenon of transport by isolated vortices.

II. Hamiltonian Maps

The typical pathway for theoretically studying transport is to determine $\vec{u}_E$ and then use (1) to study the Lagrangian behavior of fluid parcels. In many situations, accurately determining the Eulerian flow field is a difficult task in its own right. Laboratory measurements and geophysical observations are often too sparse to determine $\vec{u}_E$ over a large region. For simple flow situations one may be able to determine the Eulerian flow analytically through such tools as bifurcation theory. In the case of complex flows, however, one must usually resort to numerical simulation.

Even if one knows the Eulerian flow, studying transport requires integrating (1) for a long time using a large number of initial conditions. These computations, even for a single set of flow parameters, can often be too expensive to be currently practical. In this paper we discuss the use of Hamiltonian maps to efficiently calculate transport properties of two-dimensional structured flows. One such map has been previously used to study transport in waves [5, 6]. Here we present the viewpoint that this technique is applicable to a wider variety of structured flows, with each class of structures requiring a different specific Hamiltonian map.

The relationship between Hamiltonian dynamics and transport is due to the incompressibility of the flow [7]. In incompressible two-dimensional flows the Eulerian velocity $\vec{u}_E = u\hat{x} + v\hat{y}$ is determined by a streamfunction $\psi(x, y, t)$:

$$u = -\partial\psi/\partial y, \quad v = \partial\psi/\partial x. \tag{2}$$

Equations (1) and (2) imply that the parcel trajectories $\vec{X} = x\hat{x} + y\hat{y}$ are given by Hamilton's equations with ψ acting as the Hamiltonian:

$$\dot{x} = -\partial\psi/\partial y, \quad \dot{y} = \partial\psi/\partial x. \tag{3}$$

The entire theory of Hamiltonian dynamics can now be applied to questions of transport in two-dimensional incompressible flows [8]. One important fact is that if ψ is independent of time then (3) is integrable and the fluid trajectories are regular. Steadily propagating patterns are also integrable since the streamfunction is stationary in a moving reference frame. If an integrable streamfunction has fixed points connected by a separatrix (i.e. a homoclinic or heteroclinic connection) then a periodic perturbation will typically result in chaotic fluid trajectories. Furthermore, the chaos will have the usual fractal structure of resonant islands, KAM curves, and cantori. An interesting aspect of this is due to the fact that the phase space in (3) is the physical space of the fluid. Thus, the phase space structures appear in the fluid itself and can be observed experimentally [8].

It is often the case that a pure idealized fluid structure can be described by a stationary or steadily propagating streamfunction. The transport due to this idealized structure is not too difficult to discern, as the streamfunction is integrable and the trajectories are regular. If the amplitude of a structure becomes sufficiently large, then the streamfunction can undergo a bifurcation creating fixed points connected by separatrices, and the separatrices can divide the fluid into regions which have very different transport behavior. For example, if the amplitude of a single frequency traveling wave is sufficiently large, then the fluid is divided by a separatrix into two regions: a region where parcels are trapped by the wave and carried long distances, and a region where parcels flow backwards with respect to the wave [9]. Two parcels starting nearby, but on different sides of the separatrix will thus have very different fates.

An important point is that the qualitative nature of transport by fluid structures is determined by the topology of the separatrices in the time-independent idealized structure, i.e. how the separatrices are connected to each other. Geometrical features such as the exact shape or location of a separatrix will only affect quantitative aspects of the transport. Thus, one has a certain freedom in characterizing the streamfunction of a structure. As long as a streamfunction correctly captures the topology of separatrices it will qualitatively reproduce the transport. Additionally, if the streamfunction's geometry can be varied by changing parameters then one can study how quantitative aspects of transport

depend on the geometry. Thus, one can profitably study transport using an approximate streamfunction, bypassing the difficulty of accurately determining the Eulerian flow.

Once the idealized structure is modeled by an integrable streamfunction the next step is to study the effect of perturbations. Here we use the hypothesis that the chaotic behavior of weakly perturbed integrable Hamiltonian systems is relatively insensitive to the details of the perturbation. This hypothesis is extremely useful in that it both allows one to choose particularly convenient perturbations and it frees one from having to study in detail the types of perturbations which affect a given structure in its natural environment. By carefully choosing a periodic perturbation one can obtain a system which can be analytically integrated over a single period of the perturbation, transforming the original set of Hamiltonian ordinary differential equations into a Hamiltonian map. This is advantageous since it is significantly easier and faster to compute iterations of maps than integrations of ordinary differential equations. This procedure was originally used to study chaotic behavior in the pendulum where it results in the standard map [10, 11].

While the hypothesis of insensitivity to details of the perturbation is certainly true for periodic perturbations, it is unclear how valid it is for other types of perturbations. Beigie, et.al. [12], studied transport in quasiperiodically perturbed flows, and discussed how their ideas apply to more general perturbations. Babiano, et.al. [13], studied advection in flows with more complex time dependence, looking at both collections of point vortices, whose motion is chaotic, and at two-dimensional turbulence. In all these cases, the separatrices of the unperturbed structures are found to break producing chaotic behavior. However, it is still unknown how sensitive transport behavior in chaotic regions is to the time-dependence of the perturbation. The method we present here allows one to efficiently study transport in a periodically perturbed flow. The use of this technique should help in understanding the differences between periodic and non-periodic flows.

Thus, the strategy for efficiently calculating transport in the chaotic regions of a structured flow is as follows. First, one constructs a simple time-independent streamfunction whose topology of separatrices matches those of the structure of interest. Second, one adds a periodic perturbation which can be analytically integrated, creating a Hamiltonian

map. The resulting map can then be iterated numerically for very long times, using large numbers of initial conditions, and for a wide range of parameter values.

III. Isolated Vortices

Isolated vortices appear in many regions of the Earth's ocean and play a significant role in the ocean's transport of heat and salinity. One well known type of ocean vortex is a Gulf Stream ring, created when a meander in the Gulf Stream grows in amplitude and pinches off [3]. The pinched-off meander becomes a vortex whose interior contains water that was originally on the opposite side of the jet. Since the Gulf Stream acts as a barrier to heat and salinity transport, these vortices provide a mechanism for transport across the jet. Gulf Stream rings typically have diameters of a few hundred kilometers, and lifetimes of 1-4 years. Similar vortices also detach from intense currents in other parts of the ocean. Another type of vortex, called a Meddie (Mediterranean eddie), is found in the North Atlantic and is associated with outflow from the Mediterranean Sea [14]. Meddies have large heat and salinity anomalies, diameters of about 100 km, and have been tracked for up to 2 years. It is thus of great geophysical interest to learn how water is exchanged between the interior and exterior of isolated vortices.

Isolated vortices on the Earth travel westward due to the "beta-effect", the variation in the Coriolis force with latitude [15, 16]. In a frame comoving with the vortex, the streamfunction of an idealized vortex has a single fixed point with a homoclinic orbit [4] (Figure 1). Fluid parcels inside the homoclinic orbit are trapped and carried with the vortex while parcels outside are left behind by the vortex. Parcels outside the vortex but on the stable manifold of the fixed point are carried with the vortex forever, but these parcel form a set of measure zero and are not significant. What is significant is that parcels close to the stable manifold slow down (in the comoving reference frame) on approaching the fixed point and are thus carried with the vortex for a while before being left behind.

Ocean vortices are subject to a variety of perturbations: they emit Rossby waves as they propagate producing a periodic perturbation, they exist in a turbulent background flow, and they propagate over a complex topography. It is expected that these perturbations break the homoclinic orbit and produce chaotic trajectories. While the transport

due to an unperturbed vortex has previously been considered [4], the impact of the chaotic trajectories has not to our knowledge been studied.

To construct a Hamiltonian map for an isolated vortex, a "vortex map", we start with the streamfunction for an unperturbed vortex. Many quantitatively different but qualitatively similar streamfunctions have been used to study isolated vortices [17, 18, 19]. Here we choose a Gaussian streamfunction, used in [17] as their standard profile, which has the advantage of having zero net circulation and hence leaves the flow unaffected at infinity. We assume the vortex has amplitude A and is propagating westward (towards negative x). In a frame comoving with the vortex the streamfunction is

$$\psi_0(x, y) = Ae^{-(x^2+y^2)} - y, \tag{4}$$

where distances are measured in units such that the vortex size is unity and time is measured in units such that the propagation speed is unity. The streamfunction undergoes a saddle-node bifurcation when $A = A_c = e^{1/2}/\sqrt{2} \approx 1.16$; below A_c there are no fixed points while above A_c there is a stable fixed point at $x = 0$, $y = y_s$ and an unstable fixed point at $x = 0$, $y = y_u$. The fixed points are solutions of $2Ay\exp(-y^2) = 1$ and $y_u < y_s$. The existence of closed streamlines and stagnation points in ocean vortices indicates that they have amplitudes above the bifurcation value. Figure 1 shows ψ_0 for $A = 2.0$.

The next step is to pick a periodic perturbation ψ_1 that allows the explicit construction of a map. This can be done if the addition of ψ_1 results in a streamfunction which has separate terms acting at different times, each of which can be analytically integrated. One perturbation which accomplishes this is:

$$\psi_1(x, y, t) = Ae^{-(x^2+y^2)} \left(k \sum_{n=-\infty}^{\infty} \delta(t - nk^+) - 1 \right), \tag{5}$$

where δ denotes the Dirac delta function, and nk^+ denotes letting the delta-function act at time $nk+\epsilon$ and taking the limit $\epsilon \to 0$ after doing the integration. The total streamfunction, $\psi = \psi_0 + \psi_1$ is

$$\psi = Ake^{-(x^2+y^2)} \sum_{n=-\infty}^{\infty} \delta(t - nk^+) - y, \tag{6}$$

which is of the form described above since the exponential part only acts at times $t = nk^+$, and the linear part acts during the remainder of the time.

In Cartesian coordinates the equations of motion (3) cannot be integrated through the delta-function because the equations are coupled and require the value of x and y at the time the delta-function acts. In polar coordinates, however, the equations of motion are

$$\begin{aligned} \dot{r} &= \cos\theta, \\ \dot{\theta} &= -2Ake^{-r^2} \sum_{n=-\infty}^{\infty} \delta(t - nk^+) - \sin\theta/r, \end{aligned} \tag{7}$$

and the delta-function appears only in the $\dot{\theta}$ equation with an amplitude that depends only on r. To integrate the equations from $t = nk$ to $t = (n+1)k$ one first integrates in polar coordinates from $t = nk$ past the delta-function to, say, $t = nk + 2\epsilon$ resulting in

$$\begin{aligned} r(nk + 2\epsilon) &= r(nk) + O(\epsilon), \\ \theta(nk + 2\epsilon) &= \theta(nk) - 2Ake^{-r^2(nk)} + O(\epsilon). \end{aligned} \tag{8}$$

Transforming back to Cartesian coordinates, integrating to $t = (n+1)k$, and letting $\epsilon \to 0$ results in the vortex map:

$$\begin{aligned} x_{n+1} &= r_n \cos(\theta_n - 2Ake^{-r_n^2}) + k, \\ y_{n+1} &= r_n \sin(\theta_n - 2Ake^{-r_n^2}), \end{aligned} \tag{9}$$

where the subscript n refers to quantities at $t = nk$.

The streamfunction ψ_1 is, in the limit $k \to 0$, a small-amplitude, high-frequency perturbation to ψ_0. In addition, ψ_1 is a perturbation in the sense that for small k the map (9) is a finite difference approximation to the equations of motion given by ψ_0 alone. Both the standard map [10, 11] and the traveling wave map [5] are obtained by adding the same type of perturbation. Note that unlike the standard map and the traveling wave map, the vortex map is neither periodic in x nor y.

For very small k the vortex map, like other chaotic maps, has very thin chaotic layers which grow as k increases. The chaotic layer which has the most significant impact on transport is the one that appears around the stable and unstable manifolds of the unstable fixed point. This chaotic separatrix layer is due to the breaking by the perturbation of

the homoclinic orbit in ψ_0, resulting in intersections of lobes of the manifolds creating a homoclinic tangle [11, 20]. Figure 2 shows iterations of the vortex map (9) for initial conditions in the separatrix layer. The sharp boundary of the chaotic region due to KAM curves and the existence of islands and lobes is clearly seen. The importance of the separatrix layer is that it allows the vortex to trap and release fluid parcels, a phenomenon which is absent in ψ_0. The trapping manifests itself by parcels rotating about the core of the vortex for a while before being released. Since the vortex is propagating, this trapping results in spatial transport of fluid parcels.

The transport in regions outside the chaotic layer is essentially unchanged from the unperturbed case. Inside the vortex there remains a core of fluid where particles are permanently trapped, while far from vortex particles flow past the vortex without ever being trapped. These regions both have chaotic layers, but they do not affect the trapping behavior of the vortex. The core of permanently trapped fluid is similar to that seen by Babiano, et.al. [13], in more complex flows. The size of the core decreases as the separatrix layer grows.

In what follows, we shall study the dependence of transport in the separatrix layer on the the amplitude of the perturbation k and amplitude of the vortex A. As we are concerned with the effects of small perturbations on the vortex, we shall only investigate k up to 0.7.

The trapping time $\tau(y; x_0, x_1)$ is defined as the time $\tau = n_t k$, where n_t is the number of iterations for a parcel starting at (x_0, y) to reach x_1. If x_0 and x_1 are on either side of the vortex then τ is a good measure of the time spent being carried by the vortex. Figure 3 shows one example of $\tau(y)$. One sees multiple peaks where parcels are trapped for very long times, separated by regions where parcels travel relatively quickly through the vortex. The peaks are distributed in a self-similar manner typical of structure in chaotic regions.

Using $\tau(y)$ and defining a threshold τ_0 allows measurement of the width of the chaotic layer: $w = y_1 - y_0$, where y_1 and y_0 are, respectively, the largest and smallest y with $\tau(y) > \tau_0$. We find that the measured width is relatively insensitive to τ_0 for τ_0 sufficiently large. Figure 4 shows $w(k)$ for three values of A, indicating that the width grows with both k and A. At smaller values of k, the growth of w is extremely fast.

As a vortex travels through the fluid it picks up parcels, carries them a while, and deposits them elsewhere. The final spatial distribution in x of an initial small region of fluid is given by the distribution of trapping times $p(\tau)$, with the speed of the vortex providing the transformation between time and distance. Figure 5 shows the distribution of trapping times for $A = 2.0$ and a range of k. The distributions show a significant amount of structure and appear to be composed of many individual steep exponentials which merge together at larger τ resulting in a shallow exponential tail. This merging occurs at smaller τ for larger k. The separate exponentials all appear to have the same slopes, and the slope of the tail appears independent of k.

Figure 6 shows $p(\tau)$ for a range of A at fixed k. One sees that the slopes of both the individual exponentials and the smooth tails are roughly independent of A. At lower A the individual exponentials remain well resolved out to larger τ.

A flow with a single unstable periodic orbit, such as ψ_0 with its unstable fixed point, results in a $p(\tau)$ with a single exponential. The slope of that exponential for ψ_0 matches that of the steep exponentials in Figures 5 and 6. We conjecture that the individual steep exponentials can each be associated with the slowing down due to a single periodic orbit in the chaotic layer. Since the Smale horseshoe producing the chaotic layer has an infinite number of periodic orbits with orbits of all periods [21] one expects the fine structure of $p(\tau)$ to be quite complex. The connection between periodic orbits and transport is currently an active area of investigation, see for example [22, 23]. The constancy of the slopes in Figures 5 and 6 indicates that in some sense the structure of the periodic orbits is independent of both A and k. This raises the possibility that not only is the qualitative phenomenon of trapping independent of the details of the vortex and perturbation, but that some quantitative aspects such as the slopes in $p(\tau)$ are also robust.

IV. Discussion

Understanding the transport properties of structured flows is extremely important to many geophysical problems. The method described here of constructing Hamiltonian maps should provide a useful tool for the first step in reaching such understanding. However the method is only a first step in that the map is a significant simplification of the true flow.

First, the resulting maps are kinematic, in that they use an assumed Eulerian evolution, rather than the true dynamic evolution of the flow. Indeed, the simple flows which allow the explicit construction of maps are typically not solutions of the Eulerian dynamical equations. The validity of the approach rests on the ansatz that the chosen flow captures those aspects which are important to transport: the topology of the streamlines in the time-independent idealized structure, and the existence of small perturbations. Second, the maps are two-dimensional, and thus exclude any structures where the third dimension is important for transport. The degree to which transport under the true Eulerian evolution in both two and three-dimensional flows differs from that in simple Hamiltonian maps is an important question which must be investigated.

There is evidence, however, that Hamiltonian maps do capture some important aspects of transport. del-Castillo-Negrete and Morrison [6] used a Hamiltonian map to reproduce the transport seen in laboratory experiments on Rossby waves in rotating fluids [24]. Laboratory experiments of vortices on a β-plane [18] show similar behavior to the above vortex map (9). In particular, the lobes seen in their experiment match the lobes found in homoclinic tangles and visible in the vortex map (Figure 2). However, the lobes in the experiment contain potential vorticity, an active rather than passive tracer, and the lobes subsequently roll up into secondary vortices. This roll-up is absent from the vortex map due to the purely kinematic aspect of the formulation. Thus, while kinematic Hamiltonian mappings are only an approximation to the true behavior of fluid structures, they are relatively simple to construct for a variety of structures and allow one to efficiently calculate transport properties.

V. Acknowledgements

The National Center for Atmospheric Research is sponsored by the National Science Foundation.

VI. References

1. A.S. Bower and T. Rossby, J. Phys. Oceanogr. **19** (1989) 1177.

2. Michael E. McIntyre, in *Dynamics, Transport, and Photochemistry in the Middle Atmosphere of the Southern Hemisphere*, A. O'Neill, ed., p.1 (Kluwer Academic Publishers, Dordrecht, 1990).

3. P.L. Richardson, in *Eddies in Marine Science*, A.R. Robinson, ed., p.19, (Springer-Verlag, Heidelberg, 1983).

4. William K. Dewar and Glenn R. Flierl, Dyn. Atmos. Oceans **9** (1985) 215.

5. Jeffrey B. Weiss, Phys. Fluids A **3** (1991) 1379.

6. Diego del-Castillo-Negrete and P.J. Morrison, Phys. Fluids A (1993) 948.

7. Hassan Aref, J. Fluid Mech. **143** (1984) 1.

8. J.M. Ottino, *The kinematics of mixing: stretching, chaos, and transport*, (Cambridge University Press, Cambridge, 1989).

9. E. Knobloch and J.B. Weiss, Phys. Rev. A **36** (1987) 1522.

10. B.V. Chirikov, Phys. Rep. **52** (1979) 265.

11. A.J. Lichtenberg and M.A. Lieberman, *Regular and Stochastic Motion*, (Springer-Verlag, New York, 1983).

12. Darin Beigie, Anthony Leonard, and Stephen Wiggins, Nonlinearity, **4**, 775, (1991).

13. A. Babiano, G. Boffetta, A. Provenzale, and A. Vulpiani, preprint.

14. P.L. Richardson, D. Walsh, L. Armi, M Schröder, and J.F. Price, J. Phys. Oceanogr. **19** (1989) 371.

15. James C. McWilliams and Glenn R. Flierl, J. Phys. Oceanogr. **9** (1979) 1155.

16. Richard P. Mied and Gloria J. Lindemann, J. Phys. Oceanogr. **9** (1979) 1183.

17. Peter R. Gent and James C. McWilliams, Geophys. and Astrophys. Fluid Dyn. **35** (1986) 209.

18. G.F. Carnevale, R.C. Kloosterziel, and G.J.F. van Heijst, J. Fluid Mech. **233** (1991) 119.

19. X.J. Carton and J.C. McWilliams, in *Mesoscale/Synoptic Coherent Structures in Geophysical Turbulence*, Jacques C.J. Nihoul and Bruno M. Jamart, eds., p.255 (Elsevier, Amsterdam, 1989).

20. S. Wiggins, *Global Bifurcations and Chaos*, (Springer-Verlag, New York, 1988).

21. John Guckenheimer and Philip Holmes, *Nonlinear Oscillations, Dynamical Systems, and Bifurcations of Vector Fields*, (Springer-Verlag, New York, 1983).

22. Bruno Eckhardt, Phys. Lett. A **172** (1993) 411.

23. Roberto Artuso, Giulio Casati, and Roberti Lombardi, Phys. Rev. Lett. **71** (1993) 62.

24. J. Sommeria, S.D. Meyers, and H.L. Swinney, Nature **337** (1989) 58.

Figure Captions

Figure 1. Streamfunction ψ_0 with $A = 2.0$.

Figure 2. Trajectories of the vortex map with $A = 2.0$ and $k = 0.5$ for 500 initial conditions starting at $x = -1.5$ and evenly spaced across the chaotic layer.

Figure 3. Trapping time $\tau(y; x_0, x_1)$ for $A = 2.0$, $k = 0.5$, $x_0 = -2.0$ and $x_1 = 2.0$.

Figure 4. Width of the chaotic layer at $x = -2.0$ using a threshold trapping time of $\tau_0 = 50$, $x_0 = -2.0$, and $x_1 = 2.0$.

Figure 5. Distributions of trapping times $p(\tau)$ for $A = 2.0$, $x_0 = -2.0$, $x_1 = 2.0$ and a range k, each computed from 10^6 initial conditions evenly spaced in y. The bins in the histograms have a width of one iteration, $\Delta t = k$. Successive distributions are shifted vertically to ease comparison.

Figure 6. Same as Fig.5, but for $k = 0.6$ and a range of A.

Figure 1

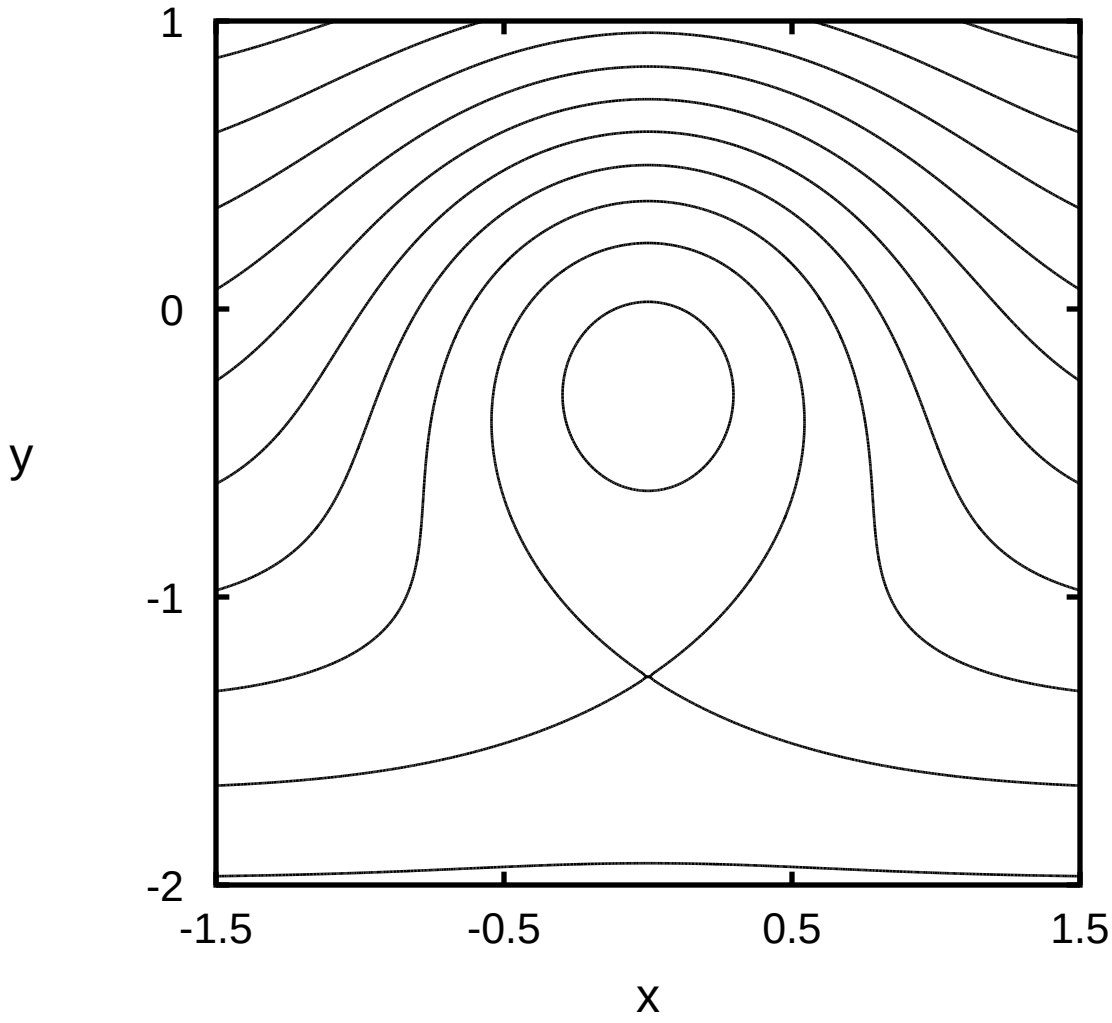

Figure 2

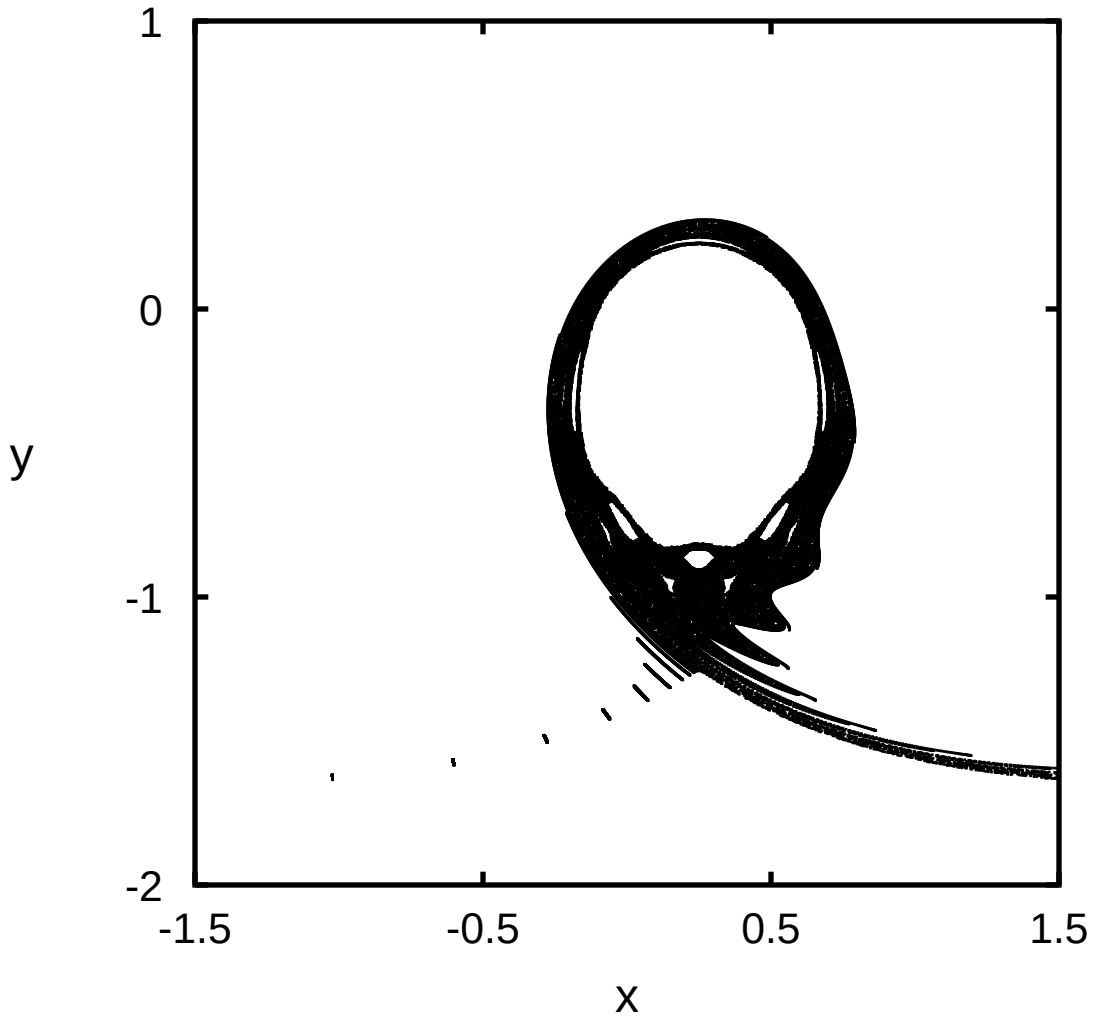

Figure 3

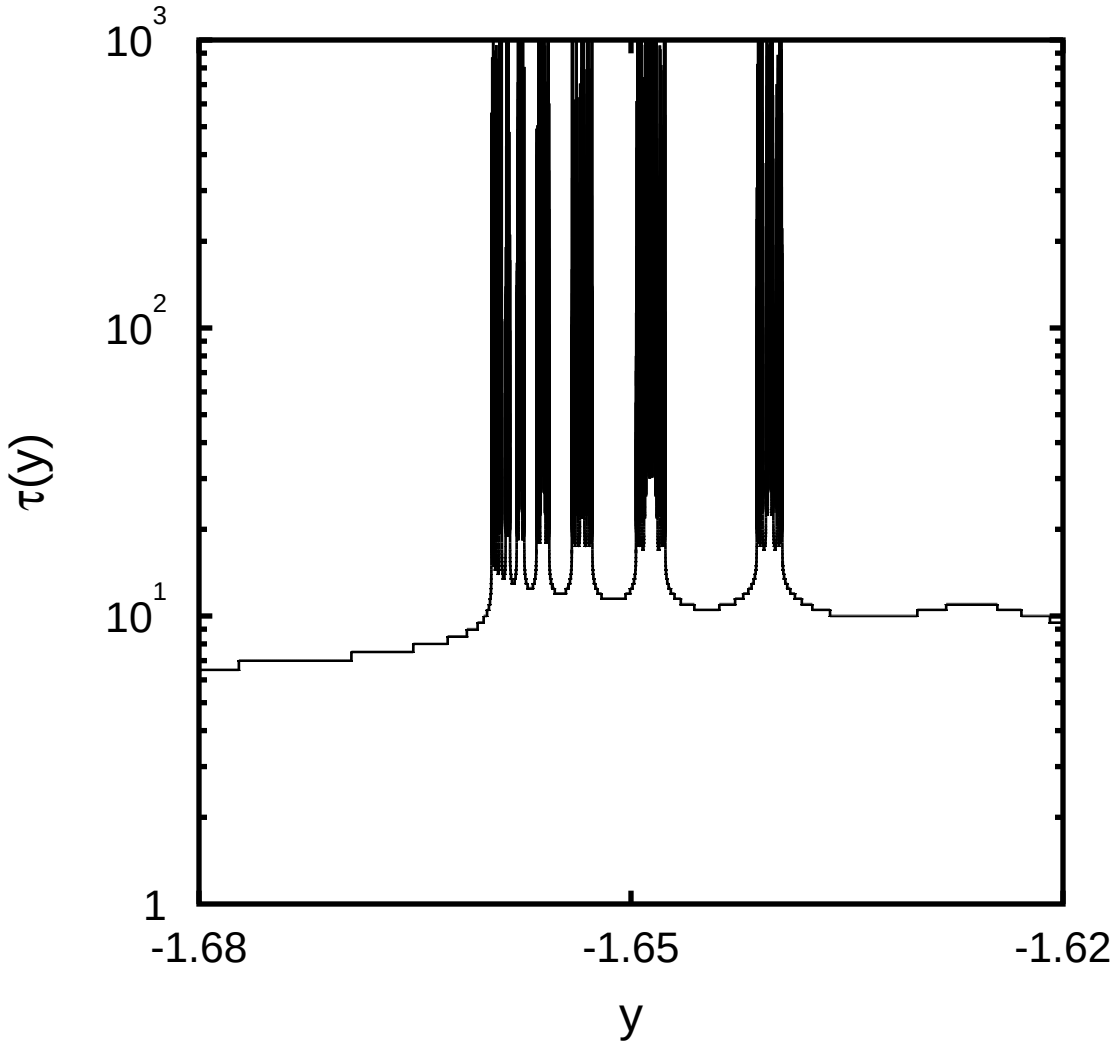

Figure 4

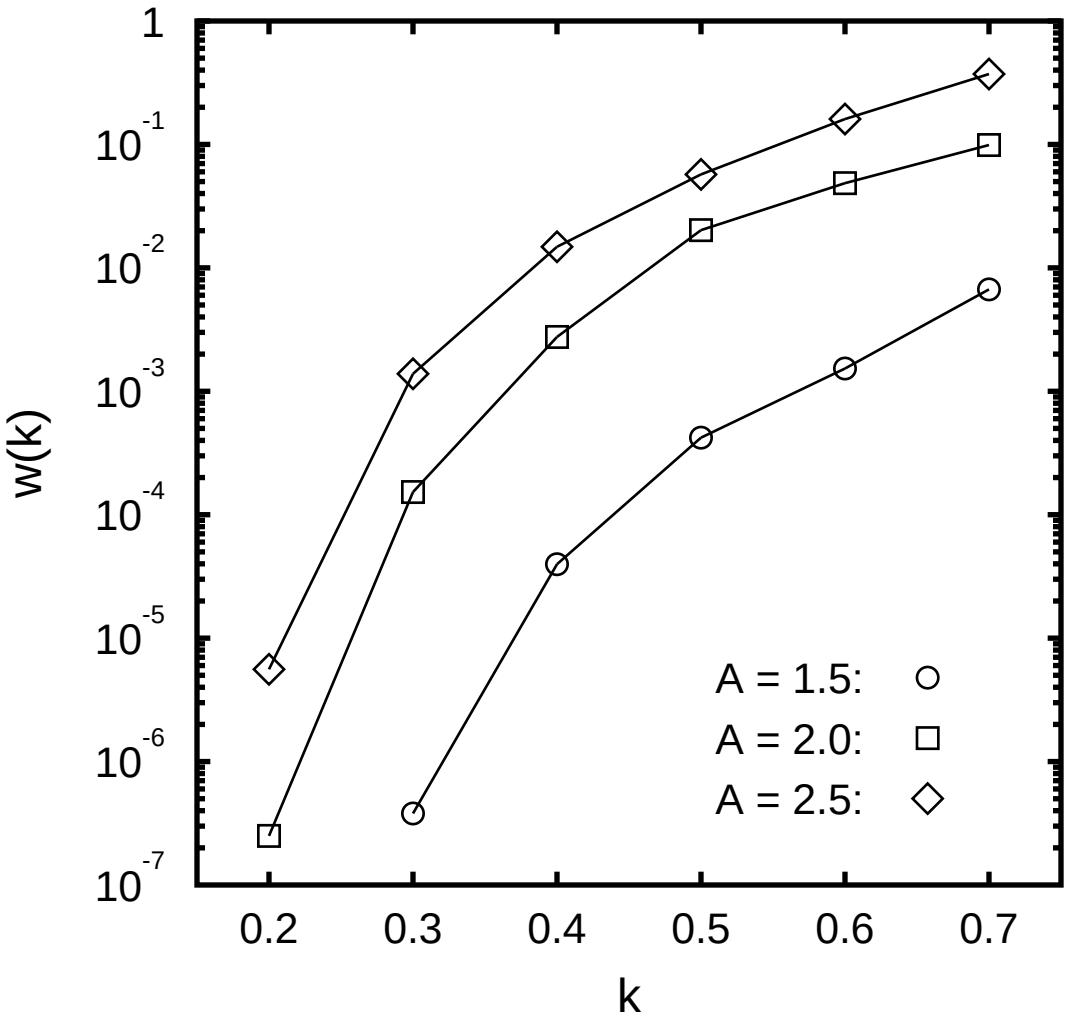

Figure 5

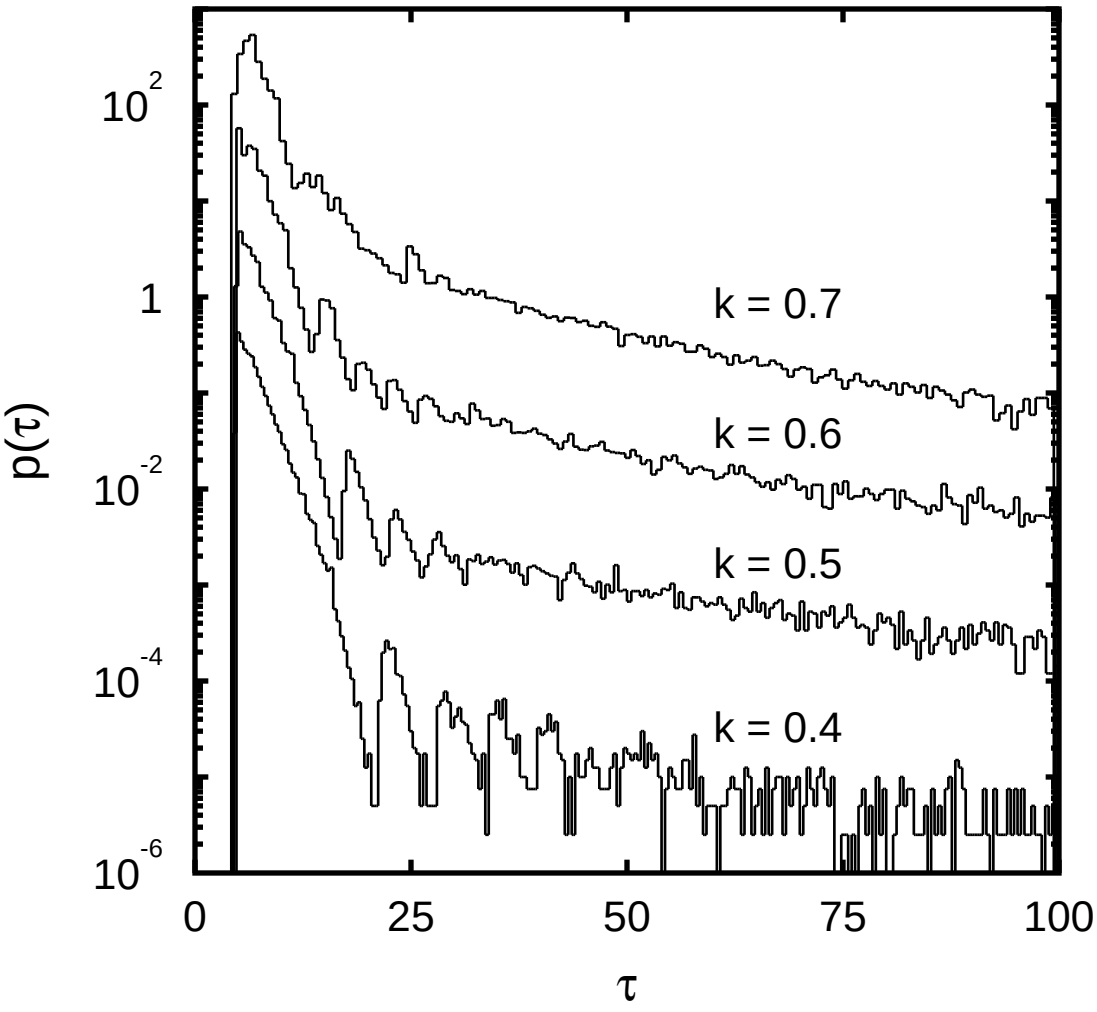

Figure 6